BR14 - The Effects of Bauxite Residue on Mechanical and Architectural Properties of Portland Cement-Based Compositions

Roberto Cesar de O. Romano[1], Markus S. Rebmann[2], Juliana M. Neves[3], Marcelo Montini[4], Raphael Costa[5] and Rafael G. Pileggi[6]

1. Researcher
2. Researcher
3. Researcher
6. Full Professor

University of São Paulo, São Paulo, Brazil

4. Senior Chemical Consultant,
5. Head of Technology

Norsk Hydro, Barcarena, Brazil

Corresponding author: rcorjau@gmail.com

Abstract

One of the most promising large-scale applications of bauxite residue of Bayer process (BR) is its direct addition in concrete composites. Over the past years, efforts have been made towards developing concrete mixtures proportions that fit the purpose to which they are intended for, including cladding, pavers, and monolithic concrete for light and heavy traffic. In addition to the feasibility of mixing and placing these concrete mixtures, i.e., understanding their rheology, it is of primary importance to evaluate their hardened characteristics as a function of BR content. This research comprises the evaluation of six mortar mixtures corresponding to the mortar fraction of the developed concrete mixtures, with partial replacement of sand by BR. The range of sand replacement by BR was based on the volume of cement and varied from 5 to 50 %, while keeping constant the cement content among the mixtures. The mechanical evaluation includes measurements of uniaxial compressive strength and elastic modulus, whereas color and efflorescence were evaluated for architectural purposes. In addition, the effect of BR replacement was evaluated in terms of water absorption by capillary porosity, a parameter that directly affects mass transport and durability of concrete components.

Keywords: Bauxite residue, Color, Mechanical properties, Capillarity and Efflorescence.

1. Introduction

The aluminum industry is actively engaged in exploring options to decrease both the volume of generated bauxite residue (BR) and the associated land area required for its storage. A crucial facilitator of this initiative involves the identification and development of opportunities for value adding uses of BR.

However, even with over 100 years of research, hundreds of publications and more than 3000 patents filed, the reuse of BR remains notably limited, reaching only around 4 % of the total generated volume. This constrained uptake can be attributed to several primary technical obstacles, including the elevated salinity, the occurrence of heavy and alkaline metals, and in certain instances, the presence of radioactive elements within the BR. Also, part of this barrier is the low costs of disposal, which typically ranges from $4 to $12 per ton of residue. However, the global demands of sustainability are increasing the speed for the search for applications that consume a large amount of the waste, aiming to considerably decrease, or even exhaust the entire world generation of BR.

The construction and infrastructure sector hold significant potential for addressing the issue of waste generated from various mining processes [1,2]. Given the increasing attention on sustainable methodologies and environmental awareness, the importance of waste handling and repurposing has grown significantly.

At present, the worldwide production of bauxite residue stands at approximately 160 million tons per year, which constitutes less than 4 % of the total global output of Portland cement, surpassing 4 billion tons annually. This notable contrast underscores the substantial potential for the current Portland cement production to absorb and utilize BR as a supplementary material.

The compatibility between BR and different types of Portland cement, as evidenced by recent literature, is a crucial aspect [2–7]. The high content of aluminum, silicon, and iron in BR makes it suitable for incorporation into cement compositions. These elements are essential constituents of cementitious materials, and their presence in BR suggests that it can serve as a potential raw material for cement production.

Our investigations, conducted over the last 15 years, have demonstrated the technical viability of employing bauxite residue sourced from various locations in Brazil [8–12]. The inclusion of bauxite residue in cement compositions holds the promise of delivering multiple benefits; however, it also holds the potential to compromise certain aspects concerning performance and durability.

Furthermore, according to the report of the Roadmap of International Aluminium Institute [13], the elevated alkali levels in supplementary cementitious materials (SCM) used alongside Portland cement must be carefully managed to prevent the potential for significant efflorescence. Although not intrinsically harmful, the aesthetic implications are deemed unacceptable. Therefore, the consequences of alkali contained in BR must be examined on a case-by-case basis. However, the evaluation of the aspects related to the architectural application of some compositions developed with BR is still poorly investigated [14,15].

So, the main purpose of this work was to evaluate the influence of incorporating varying amounts of bauxite residue (BR) on the mechanical properties as well as the visual architectural attributes of the produced cementitious compositions. Importantly, this evaluation was conducted while maintaining a constant cement consumption throughout the experiments.

2. Materials and Compositions

Bauxite residue (BR) from the Hydro alumina refinery located at Barcarena, state of Pará, Brazil, was used to produce the cementitious compositions. A high clinker content Brazilian Portland cement (CPV), which is equivalent to CEM I according to European standards or Type III in the US Standard, along with quartz sand, was selected for this purpose. This selection was made due to their widespread use in concrete plants situated near the location where the bauxite residue is generated, taking into account the logistical considerations pertinent to this study. As water reducer a midrange plasticizer (Mira Set 63 - GCP Chemicals) was incorporated. The primary physical characteristics of the raw materials are detailed in Table 1 while the chemical composition of both the cement and bauxite residue is provided in Table 2.

The particle size distribution of bauxite residue (BR) is notably broader in comparison to that of Portland cement, characterized by a d_{90} value of approximately 85 μm, while the binder's d_{90} value was around 45 μm. This disparity is attributed to the utilization of BR in its original form, without undergoing any form of treatment such as grinding or sieving, prior to its application. An additional noteworthy aspect pertains to the elevated volumetric surface area (product between specific surface area and specific gravity). The higher this value, the higher the water demand to

cover particle surface, resulting in a reduced quantity of free water available to create separation between adjacent particles. Consequently, the higher the BR consumption, the higher the viscosity and yield stress of compositions in the fresh state.

The sodium content of BR deserves to be highlighted. Given that this waste underwent dewatering via a press filter, initial expectations leaned towards a reduced sodium quantity. The potential consequences of an unfavorable chemical interaction between cement and BR are noteworthy, as it may lead to a significant release of this alkali into the surrounding environment. This has the potential to impose constraints on the ability to escalate the incorporation of BR within the compositions. Sodalite was the main phase of this element determined by X-ray diffraction.

Aluminum and iron were also observed in high level in the BR, due to the presence of gibbsite, goethite, and hematite. Hence, the loss on ignition of approximately 8.40 can be attributed to the thermal decomposition of water originating from gibbsite and goethite, as revealed by thermogravimetric analysis (TGA). This interpretation is supported by the absence of carbonate within this sample.

Table 1. Main physical characteristics of raw materials.

Material	D_{10} (µm)	D_{50} (µm)	D_{90} (µm)	Specific gravity (m^2/g)	Specific surface area (m^2/g)	Volumetric surface area (m^2/g)
Cement	4.90	17.1	44.7	3.19 ± 0.01	1.56 ± 0.14	4.98
BR	1.60	7.50	85.0	2.98 ± 0.04	7.74 ± 0.72	23.1
Quartz Sand	182	327	926	2.66 ± 0.02	-	-

Table 2. Chemical composition of cement and bauxite residue.

Material	SiO_2	CaO	Al_2O_3	Fe_2O_3	SO_3	MgO	Na_2O	K_2O	P_2O_5	TiO_2	LOI
Cement	17.8	61.8	4.35	4.08	2.29	3.18	0.06	0.34	0.14	0.24	4.85
BR	16.3	1.15	***22.1***	***36.2***	-	<0.10	***9.72***	0.03	0.05	5.27	8.40

Table 3 illustrates the consumption of each raw material in the compositions, in kg/m^3. The water-to-cement ratio was kept constant at 0.53, while the proportion between bauxite residue and cement was varied, ranging from 5 to 50 %. Six compositions were examined, denoted as Ref, BR-5, BR-10, BR-20, BR-30, and BR-50. The approach undertaken in this work aimed to maintain a constant cement consumption while increasing the utilization of bauxite residue; this was achieved by proportionally reducing the inclusion of quartz sand. It is noteworthy to mention that there existed a negligible alteration in the absolute values of cement consumption. This discrepancy arises due to the calculations being grounded on the material required for generating 1 cubic meter of the product, and a slight variance in the air content introduced into the compositions contributed to this minimal difference. The cementitious compositions featured nearly uniform plasticizer dosages due to the unvarying cement content, leading to differing rheological characteristics across the mortars. The cementitious compositions featured nearly uniform plasticizer dosages due to the unvarying cement content, leading to differing rheological characteristics across the mortars. Subsequently, these modifications in the fresh-state properties were quantitatively assessed and measured as outcomes of this experimental setup.

Compositions were mixed in a Pheso (Calmetrix) rheometer, a choice made to facilitate the monitoring of fresh-state properties from the initial interaction between water and powder. The process consisted of introducing the pre-homogenized powder into the bowl and subsequently introducing water (+ midrange plasticizer), regulating the flow rate at 90 grams per second. The mixing stage was conducted for a duration of 5 minutes.

Table 3. Compositions evaluated, in kg/m³.

Sample	Cement	Bauxite residue	Quartz Sand	Plasticizer	Water	Paste volume *
Ref	588	-	1175	5.3	311	43.5%
BR-5	589	27.5	1153	5.3	312	44.7%
BR-10	594	55.5	1139	5.3	315	46.0%
BR-20	597	112	1095	5.4	317	48.5%
BR-30	590	165	1032	5.3	313	51.0%
BR-50	594	278	941	5.3	315	55.9%

** represents the percentual volume of cement + BR + plasticizer + water in the total volume of concrete*

Following the mixing phase, test specimens were fabricated in accordance with the desired testing protocols, and subsequently subjected to a 28-day curing period at a temperature of 23 °C. During this curing period, stringent measures were taken to ensure an adequately humid environment that prevented any direct contact between water and the specimens. This precautionary approach was undertaken to prevent premature leaching of soluble ions within the compositions. To achieve this, the specimens were placed within trays containing plastic cups filled with water, and these trays were then enclosed within sealed plastic bags for the duration of the curing process.

3. Methods of Tests to Evaluate the Hardened State

Color assessment was performed according to *D2244-16 - Standard Practice for Calculation of Color Tolerances and Color Differences from Instrumentally Measured Color Coordinates*, using a portable spectrometer, BYK Gardner, model "Color Guide 45/0", for color control from the perspective of the human eye. Six data collection points were defined on each piece and 3 pieces of each composition were used.

Compressive strength was determined following the Brazilian standard *NBR 5739:2018 – Concrete – Compression test of cylindrical specimens*, in an EMIC DL 10000 test machine, controlling the load rate at 490 N/s. Elastic modulus was measured according to the Brazilian *NBR 15630:2008 standard*, using a Pundit equipment.

The test to define the rate of water absorption was conducted according to *EN ISO 15148:2002. Hygrothermal performance of building materials and products – Determination of water absorption coefficient by partial immersion*. The tests were carried out in cylindrical specimens of Ø 50 mm and height of 60 mm.

The curved surface of each specimen was securely sealed using silicone glue, while retaining 3 mm gaps near the bottom face. This arrangement is designed to facilitate water penetration exclusively through the lower surface, thereby inducing a unidirectional flow towards the upper surface. Measurements of water mass absorption were taken after 15', 30', 1 h, 2 h, 4 h, 8 h, 24 h, 48 h, 72 h and 7 days.

The presence of efflorescence on the specimens was observed over a 30-day period, utilizing the same specimens employed in the water absorption tests. Photographs were captured both prior to initiating contact with water and after the completion of the testing period.

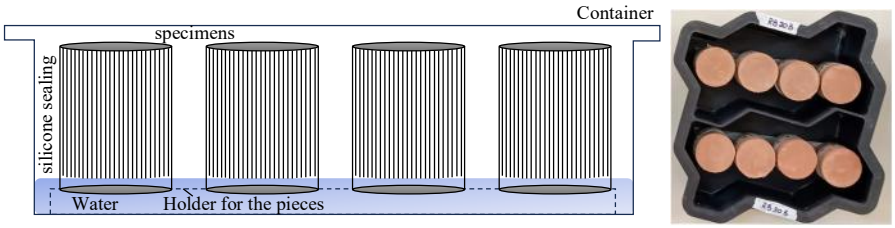

Figure 1. Illustration of the apparatus used for the capillarity and efflorescence tests. After 72 hours, the samples were left in water until 28 days, when the photographs were captured to evaluate appearance of efflorescence.

4. Results and Discussion

Figure 2 illustrates the tiles produced to evaluate the impact of BR consumption on the color of pieces, while Table 4 presents a quantification of these changes using the colorimeter. For each composition, 3 specimens of tiles were evaluated, and the measurement of color was performed in each piece. So, results presented in Table 4 allow us to compare the impact withing group and between the groups with different BR consumption.

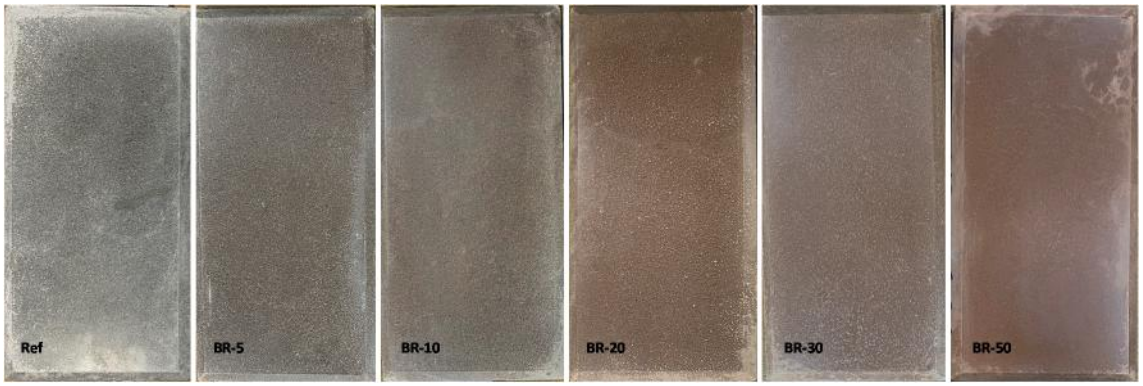

Figure 2. Tiles produced with changes in the BR consumption.

The L*ab space is a color model designed to accurately represent and describe human perception of colors. It was developed by the International Commission on Illumination (CIE) to provide a uniform and perceptually meaningful color space that can be used to quantify and communicate color differences.

The parameter ‘L’ (Lightness) represents the perceptual brightness of a color, ranging from 0 (black) to 100 (white). The ‘a’ parameter spans across negative values (green) to positive values (red), with 0 denoting neutrality on this axis. Finally, the ‘b’ parameter ranges from negative values (blue) to positive values (yellow). The L*ab color space was designed with the goal of being perceptually uniform. This means that the distance between two colors in this space more accurately corresponds to how humans perceive the distinction in color. The L*ab values provide a standardized way to quantify color differences, thereby enabling enhanced precision in color matching and control.

So, to produce pieces with BR intended for uniform color architectural applications, the control of the BR content must be precise to avoid changes in the tonality of the products fabricated across distinct batches. Conversely, in scenarios where the project embraces a spectrum of colors in its construction, such meticulous precautions might be deemed unnecessary, given that the color mosaic forms an integral part of the architectural design. After the initial color determination, these tiles underwent exposure to natural aging conditions, and the ensuing deterioration will be elucidated in forthcoming research endeavors.

Figure 3 illustrates the compressive strength (top chart) and the modulus of elasticity (bottom chart) of the samples in function of the consumption of bauxite residue. The compressive strength of concrete is a critical mechanical property that plays a central role in determining the overall performance and suitability of concrete for various applications. It is a fundamental indicator of a concrete's ability to withstand the loads and stresses that it will experience in its intended structural application. It is especially crucial for load-bearing structures like buildings, bridges, dams, and other infrastructures. On the other hand, the modulus of elasticity is an important parameter for understanding the behavior of concrete in response to various types of stresses and loads. It contributes to the safety, serviceability, and durability of concrete elements in diverse applications.

In theory, a robust correlation exists between the type and quality of Portland cement and the resulting compressive strength and modulus of elasticity, but also with other factors such as aggregate properties, water-to-cement ratio, curing conditions, use of supplementary cementitious materials, the overall mix design, and the approach adopted for casting.

Table 4. Monitoring of the color spectrum of the tiles: comparison of the pieces produced with the same BR content, and of the pieces with different residue contents.

	L*	a*	b*	CIE - L*ab color	Average
Ref (1)	47.9	0.45	4.23		
Ref (2)	55.5	0.33	5.29		
Ref (3)	47.2	0.43	4.49		
BR-5 (1)	40.0	8.37	10.65		
BR-5 (2)	40.7	8.65	10.45		
BR-5 (3)	39.7	8.90	10.77		
BR-10 (1)	45.3	12.04	13.65		
BR-10 (2)	40.9	12.52	13.29		
BR-10 (3)	40.0	12.89	13.99		
BR-20 (1)	43.1	15.89	17.65		
BR-20 (2)	44.2	16.49	18.88		
BR-20 (3)	39.6	16.21	17.42		
BR-30 (1)	44.4	17.41	19.47		
BR-30 (2)	42.8	16.78	19.23		
BR-30 (3)	38.7	19.43	19.17		
BR-50 (1)	44.6	20.01	22.57		
BR-50 (2)	39.6	21.26	21.97		
BR-50 (3)	37.5	21.45	21.29		

According to the charts presented in Figure 3, despite the decrease in the values of compressive strength and modulus of elasticity in function of the increase of bauxite residue consumption, the trends were distinct. The result of compressive strength is in accordance with the work presented by [14]. The lowest average compressive strength was achieved in the composition BR-30 (165 kg of BR per m³ of concrete), and this is, comparing with the reference a reduction of 28 % on the mechanical strength. However, the statistical evaluation showed that the reference composition is distinct of all compositions with BR, except comparing with BR-10.

The same evaluation was conducted for the modulus of elasticity. As the utilization of bauxite residue (BR) increased, a corresponding decline in the modulus of elasticity was observed.

However, when contrasting the composition with the highest BR content against the reference, the reduction amounted to a mere 10 %.

According to the Table 5, the application of a one-way ANOVA (analysis of variance) indicated significant statistical differences among the compositions [16]. Subsequent implementation of Tukey's test highlighted that compositions Ref, BR-5, and BR-10 exhibited similarity among themselves, while standing apart from the others (BR-20, BR-30, and BR-50), which shared similarities with each other.

Typically, the modulus of elasticity for quartz sand falls within a typical range of values (from 20 to 50 GPa) [17], like that for common construction materials such as concrete. Conversely, the modulus of elasticity for BR tends to span approximately 10 to 30 GPa. Consequently, by replacing sand with BR, while keeping constant water-to-cement ratio, the observed alterations align with expectations.

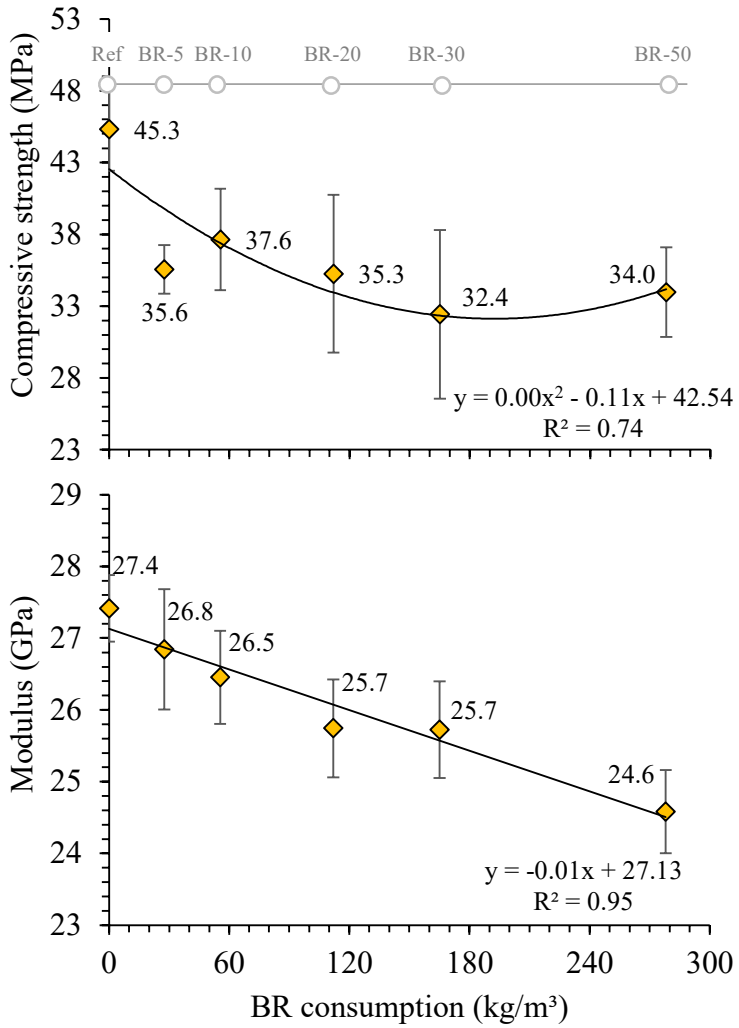

Figure 3. Compressive strength (above) and modulus of elasticity (below) of concretes in function of the BR consumption.

So, these results indicate that the use of BR directly impacted both mechanical properties, reducing them, even though the water-to-cement ratio remained constant across the various compositions.

Figure 4 depicts the monitoring of water absorption over the initial 72-hours period (on the left) while the right side illustrates the impact of varying BR content on the sorptivity at the end of the test. Capillary pores refer to small conduits that are formed as a consequence of empty spaces between aggregates and the cement paste. Even possessing microscopic dimensions, these pores enable the passage of water and other fluids through the concrete matrix.

Table 5. Statistical analysis for compressive strength and modulus of elasticity. SQ represents the sum of squares of residuals, due exclusively to random error, gl is calculated as the total number of observations minus the number of groups, MQ is the quadratic average.

One-way Anova for compressive strength

Source of variation	SQ	gl	MQ	F	p-value	F crític
Between groups	417.1	5	83.4	**5.1**	4.41E-3	**2.8**
Within groups	295.5	18	16.4			
Total	712.1	23				

Tukey's pairwise for compressive strength

	Ref	BR-5	BR-10	BR-20	BR-30	BR-50
Ref		0.032	0.127	0.025	0.003	0.010
BR-5	4.816		0.977	1.000	0.874	0.993
BR-10	3.801	1.015		0.956	0.478	0.793
BR-20	4.990	0.173	1.189		0.918	0.998
BR-30	6.376	1.560	2.575	1.387		0.994
BR-50	5.609	0.792	1.808	0.619	0.768	

One-way Anova for modulus of elasticity

Source of variation	SQ	gl	MQ	F	p-value	F crític
Between groups	29.9	5	5.98	**13.8**	5.00E-07	**2.5**
Within groups	13.0	30	0.43			
Total	42.9	35				

Tukey's pairwise for modulus of elasticity

	Ref	BR-5	BR-10	BR-20	BR-30	BR-50
Ref		0.6789	0.1367	0.0015	0.0015	0.0001
BR-5	2.0930		0.8822	0.0601	0.0601	0.0002
BR-10	3.6330	1.5390		0.4379	0.4379	0.0006
BR-20	6.2800	4.1870	2.6480		1.0000	0.0601
BR-30	6.2800	4.1870	2.6480	0.0000		0.0601
BR-50	10.4700	8.3740	6.8350	4.1870	4.1870	

Table 6 illustrates the coefficient of capillarity and time to achieve the saturation. While the first is a parameter that describes the ability (rate) of a liquid move against gravity within a narrow space, such as a small-diameter pores, due to the combined effects of adhesive and cohesive forces, the saturation time is the time to fill the volume of the specimens to the upper surface.

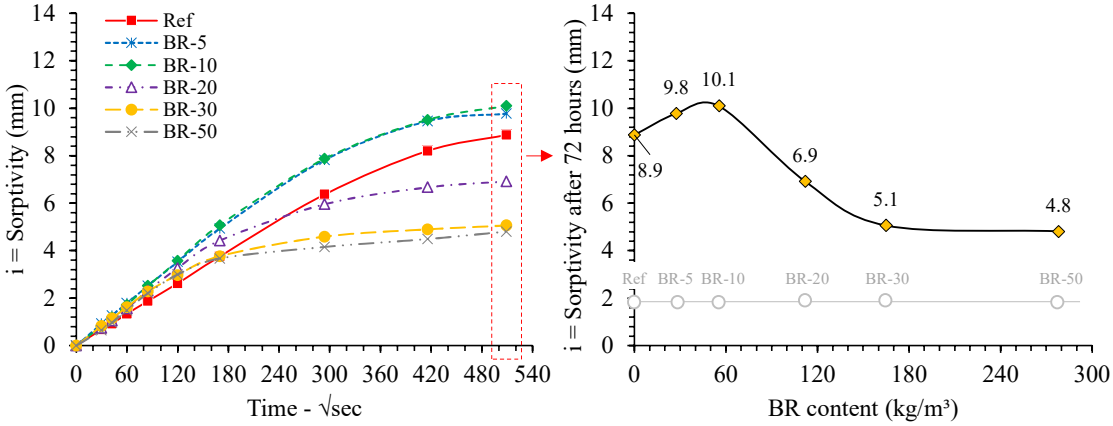

Figure 4. Water absorption over time (on the left) and comparative sorptivity after monitoring for 72 hours (on the right).

Table 6. Coefficient of capillarity and time to achieve the saturation of specimens.

	Coefficient of capillarity (mm/√sec)	Time of saturation (hour)
Ref	0.022	24
BR-5	0.029	24
BR-10	0.030	24
BR-20	0.027	8
BR-30	0.025	4
BR-50	0.026	4

The formation of capillary pores is a natural phenomenon in concrete and is directly related to the water-to-cement ratio used in the mix. A higher water-to-cement ratio can result in a greater number of capillary pores, as excess water creates voids after evaporation or concrete setting. However, for the compositions evaluated in this paper the w/c ratio was constant, illustrating that the use of BR impacted in the densification of microstructure of concretes: up to 10 % of BR there was an increase in the coefficient of capillarity while increments higher than 20 % of BR resulted in increase in the rate of penetration of water by capillarity.

Thinner pores tend to increase capillary pressure, allowing for faster percolation of water (or degrading agents in a real exposure situation). But if the tortuosity is increased, or the channels interrupted, there is interruption of absorption. The compositions with 30 and 50 % of BR stabilized faster, indicating more accentuated saturation of these specimens.

In correlation with this, the concretes featuring elevated levels of BR incorporation should probably present higher permeability. This characteristic results in an increase in the permeation of water and moisture, thereby potentially yielding an undesirable impact on the long-term deterioration of concrete and its overall durability: ingress of water carrying corrosive ions, such as chlorides, consequently contributing to the degradation of structural integrity of the material.

Another consequence of water penetration into concrete, is the occurrence of efflorescence, triggered by water seeping into the concrete and transporting dissolved salts to the surface. Upon evaporation of the water, these salts crystallize and deposit on the surface, resulting in a distinctive white, powdery formation known as efflorescence. This phenomenon is a common occurrence in concrete and can affect its visual aesthetics, thereby influencing its architectural performance.

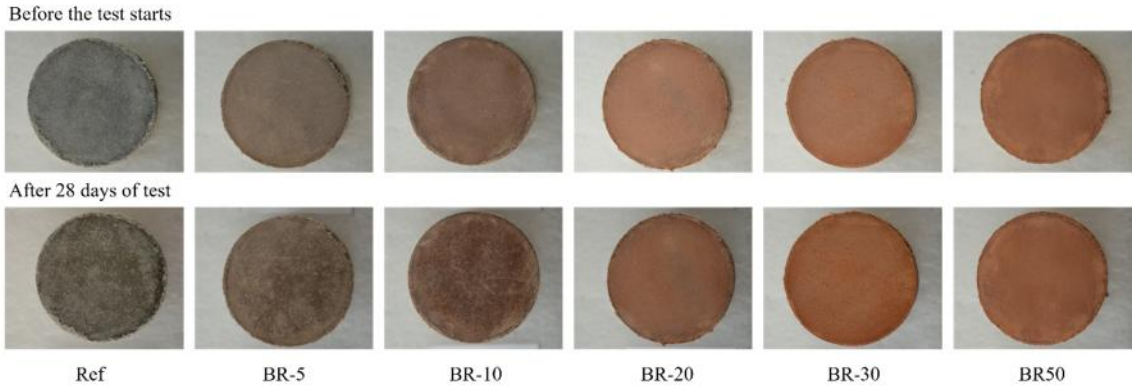

Figure 5. Monitoring of efflorescence. Above are the images captured prior to placing the specimens in contact with water, while below are the images taken after the completion of the 28-day testing period.

However, as depicted in Figure 5, no occurrence of precipitated salts on the upper surface of the specimens was observed even after a 28-day monitoring period, irrespective of the bauxite residue (BR) content incorporated in the compositions.

5. Conclusions

Alterations in the bauxite residue (BR) content within the compositions yielded products with varying color tones—some discernible to the naked eye, while others only perceivable to skilled observers or specialized color quantification equipment. Consequently, to maintain uniform color consistency across distinct batches of BR-fabricated products in architectural applications, precise control over BR content becomes imperative. Conversely, in scenarios where the project encompasses a diverse color spectrum in its construction, stringent precautions of this nature might be deemed dispensable, given the color mosaic's integration within the architectural design.

Even with a constant cement consumption (or fixed water-to-cement ratio), augmenting the BR content in the compositions resulted in a decline in both mechanical strength and modulus of elasticity. This led to a reduction of up to 28 % in rupture stress and 10 % in stiffness across the products.

A statistical evaluation pointed out, for the mechanical strength, that all compositions with BR were distinct from the reference composition, but similar to each other. In terms of modulus of elasticity, no statistically significant differences emerged between samples Ref, BR-5, and BR-10 (which exhibited similarity), while beyond this BR content, all compositions resembled each other but differed from the previous ones.

The absorption of water by capillarity indicated that up to 10 % of BR there was a decrease in the liquid percolation rate through the microstructure of the products, but for higher contents the absorption rate began to increase, changing the time for the total saturation of the specimen.

This phenomenon is of notable significance concerning the durability and architectural considerations of BR-incorporated products. The increased permeability observed in compositions with over 20 % BR indicates the potential for degrading agents' easier percolation, possibly compromising system durability. Similarly, the transport of soluble salts to specimen surfaces is plausible. However, observations spanning up to 28 days did not reveal any instances of efflorescence on the specimen surfaces.

6. References

1. K. L. Scrivener et al., Eco-efficient cements: Potential economically viable solutions for a low-CO_2 cement-based materials industry, *Cem. Concr. Res.* **114**, 2–26 (2018).
2. R. Snellings et al., Future and emerging supplementary cementitious materials, *Cem. Concr. Res.* **171**, 107199 (2023).
3. A. L. Fujii et al., Impact of superplasticizer on the hardening of slag Portland cement blended with red mud, *Constr. Build. Mater.* **101**, 432–439 (2015).
4. C. C. Liberato et al., Efeito da calcinação do resíduo de bauxita nas características reológicas e no estado endurecido de suspensões com cimento Portland, *Ambiente Construído* **12**, 53–61 (2012).
5. R. C. O. Romano et al., Hydration of Portland cement with red mud as mineral addition, *J. Therm. Anal. Calorim*. **131**, 2477–2490 (2018).
6. R. C. O. Romano et al., Combined evaluation of oscillatory rheometry and isothermal calorimetry for the monitoring of hardening stage of Portland cement compositions blended with bauxite residue from Bayer process generated in different sites in Brazil, *Rev. IBRACON Estrut. E Mater*., **14**, e14211 (2021).
7. I. Vladić Kancir and M. Serdar, Contribution to understanding of synergy between red mud and common supplementary cementitious materials, *Materials* **15**, 1968 (2022).
8. H. Choo et al., Compressive strength of one-part alkali activated fly ash using red mud as alkali supplier, *Constr. Build. Mater.,* **125**, 21–28 (2016).
9. I. M. Nikbin et al., Environmental impacts and mechanical properties of lightweight concrete containing bauxite residue (red mud), *J. Clean. Prod.,* **172**, 2683–2694 (2018).
10. Y. Pontikes and G. N. Angelopoulos, Bauxite residue in cement and cementitious applications: Current status and a possible way forward, *Resour. Conserv. Recycl*., **73**, 53–63 (2013).
11. P. S. Reddy et al., Properties and assessment of applications of red mud (bauxite residue): Current status and research needs, *Waste Biomass Valorization,* **12**, 1185–1217 (2021).
12. R. C. O. Romano et al., Impact of using bauxite residue in microconcrete and comparison with other kind of supplementary cementitious material, Proceedings of 35th ICSOBA, 2017.
13. International Aluminium Institute (IAI), *Technology Roadmap: Maximizing the Use of Bauxite Residue in Cement* (2020), p. 38
14. K. Hyeok-Jung et al., Effect of Red Mud Content on Strength and Efflorescence in Pavement using Alkali-Activated Slag Cement, *Int. J. Concr. Struct., Mater.* **12**, (2018).
15. S.-P. Kang and S.-J. Kwon, Effects of red mud and Alkali-Activated Slag Cement on efflorescence in cement mortar, *Constr. Build. Mater.* **133**, 459–467 (2017).
16. M. H. Maciel et al., Efeito da variação do consumo de cimento em argamassas de revestimento produzidas com base nos conceitos de mobilidade e empacotamento de partículas, *Ambiente Construído* **18**, 245–259 (2018).
17. A. Muqtadir et al., Elastic and mechanical properties of dune sand: experiments and nodels, *J. Geophys. Res. Solid Earth* **124**, 7978–7992 (2019).